

## Higgs self coupling: status and projections at CMS

---

**Saswati Nandan for the CMS Collaboration** <sup>a,\*</sup>

<sup>a</sup>*National Institute of Chemical Physics and Biophysics,  
Akadeemia tee 23, 12618 Tallinn, Estonia*

*E-mail:* [saswati.nandan@cern.ch](mailto:saswati.nandan@cern.ch)

Recent results on Higgs boson self-coupling,  $\lambda_{HHH}$ , performed in Higgs boson pair,  $HH$ , production in different final states are presented. The analysis is based on data recorded at a center-of-mass energy of 13 TeV by the CMS detector during LHC Run 2. Results on the non-resonant  $HH$  production cross section in different Effective Field Theory scenarios are addressed as well. A projection study for  $\lambda_{HHH}$  at the High-Luminosity LHC is also presented.

*The European Physical Society Conference on High Energy Physics (EPS-HEP2023)  
21-25 August 2023  
Hamburg, Germany*

---

\*Speaker

## 1. Introduction

Since the discovery of the Higgs ( $H$ ) boson [1–3] many of its properties have been measured. So far, all measurements are consistent with the standard model (SM) predictions. The  $H$  boson self-coupling,  $\lambda_{HHH}$ , has not yet been measured. The  $\lambda_{HHH}$  can be measured directly in  $H$  boson pair production ( $HH$ ) or indirectly through single  $H$  boson production. The main production mode of the  $HH$  process is the gluon-gluon fusion ( $GGF$ ) process (Figs. 1a, 1b), followed by the vector boson fusion ( $VBF$ ) process (Figs. 1c, 1e). In addition to these, the associated production of the  $H$  boson pair with one vector boson ( $W/Z$ ) also contributes by a small amount. The cross sections ( $\sigma$ ) of these processes are approximately 31.05 fb, 1.73 fb and 0.856 fb respectively at  $\sqrt{s}=13$  TeV [4]. While the cross section for  $HH$  production in the SM is very small, it can be enhanced in beyond the standard model (BSM) scenarios through anomalous couplings (Figs. 1f, 1h). Deviations from the SM in the value of  $\lambda_{HHH}$  and in the quartic coupling between two vector bosons and two Higgs bosons are quantified by the coupling modifiers  $\kappa_\lambda$  and  $\kappa_{2V}$ , respectively. In the Effective Field Theory (EFT) scenarios [5], signal events with similar distributions in  $m_{HH}$  and  $\cos \Theta^*$  (angle between one of the Higgs bosons and beam axis), are grouped into different benchmark (BM) points in 5D space of  $\kappa_\lambda, \kappa_{2V}, c_{2g}, c_g c_V$ . The most recent results on the measurement of  $\lambda_{HHH}$  in different final states of non-resonant  $HH$  production by the CMS [6] experiment are presented here.

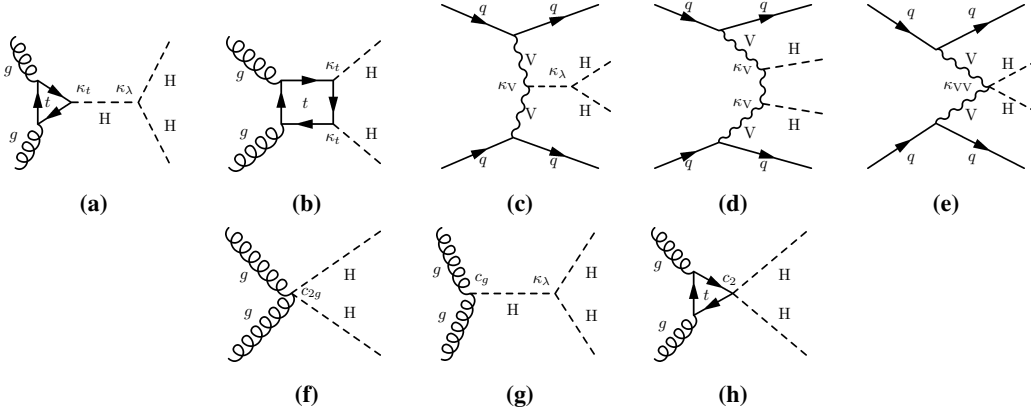


**Figure 1:** Non-resonant  $HH$  production via the  $GGF$  (a,b), and  $VBF$  (c,d,e) process and possible contributions of BSM physics via anomalous couplings (f,g,h) [7].

## 2. Boosted $HH \rightarrow bbbb$

This analysis [8] targets both  $GGF$  and  $VBF$  production modes in the region where  $b$ -tagged jets coming from two  $H$  bosons are reconstructed within two large radius jets which are reconstructed by the ParticleNet algorithm [9]. The masses of large radius jets are also regressed by the ParticleNet algorithm. A boosted decision tree (BDT) is used to separate signal and background contributions in  $GGF$  mode. Control regions (CR) are used to estimate multijet background from data. Signal regions are further split based on ParticleNet and BDT scores to increase the analysis sensitivity. A simultaneous fit of mass of the  $HH$  system in signal and CR regions is performed to extract the signal. The observed (expected) upper limit on  $\sigma(HH)$ , set by this analysis is 9.9(5.1) times SM expectation at 95% confidence level (CL) and corresponding observed (expected) upper limit on  $\kappa_\lambda$  is set within the interval  $-9.9(-5.1) < \kappa_\lambda < 16.9(12.2)$ .

### 3. $HH \rightarrow bb\tau\tau$

This analysis [10] is performed both in GGF and VBF modes and 3 final states have been studied based on leptonic and hadronic ( $\tau_h$ ) decay of  $\tau$  leptons:  $\mu\tau_h$ ,  $e\tau_h$ ,  $\tau_h\tau_h$ . Resolved and boosted categories are considered based on whether b-tagged jets coming from  $H$  boson decay are reconstructed within two small radius jets separately or in one large radius jet, respectively. The  $\tau_h$ s are reconstructed by the DeepTau algorithm [11] and the mass of  $H \rightarrow \tau\tau$  system ( $m_{\tau\tau}$ ) is reconstructed by the SVFit algorithm [12]. An elliptical cut is used on the mass of the  $H \rightarrow bb$  system and  $m_{\tau\tau}$  to reduce the background contributions in the signal regions. A multi-classifier Deep Neural Network (DNN) is used to separate GGF, VBF and other dominating background processes. The DNN distributions are used to extract the signal. The observed (expected) upper limit on  $HH$  production set by this analysis amounts to 3.3(5.2) times the SM expectation at the 95% CL and corresponding upper limit set on  $\kappa_\lambda$  is within the interval  $-1.7(-2.9) < \kappa_\lambda < 8.7(9.8)$ .

### 4. $HH \rightarrow WW^*\gamma\gamma$

The analysis in the  $HH \rightarrow WW^*\gamma\gamma$  [13] final state, targets specifically the GGF production mode. The analysis is performed in three final states based on the decay of the two  $W$  bosons: di-lepton (DL) (both  $W$ s:  $W \rightarrow l\nu$ ), single lepton (SL) ( $W \rightarrow l\nu$ ,  $W \rightarrow q\bar{q}$ ), fully hadronic (FH) (both  $W$ s:  $W \rightarrow q\bar{q}$ ). Backgrounds from multijet and  $\gamma$  + jet production are estimated from side-band regions in data, while other backgrounds are estimated from Monte Carlo simulation. The  $HH \rightarrow WW^*\gamma\gamma$  signal as well as the single  $H \rightarrow \gamma\gamma$  background are modelled by an analytic fit to the  $m_{\gamma\gamma}$  distribution while continuum background is modelled from data in the  $m_{\gamma\gamma}$  side-band region. Background contributions are removed by a cut based analysis in the DL final state, while a DNN is used in the SL and FH final states. To avoid overlap with the  $HH \rightarrow bb\gamma\gamma$  analysis [14] in the FH channel, a binary classifier is used to separate  $bb\gamma\gamma$  from  $WW^*\gamma\gamma$  events. The observed (expected) upper limit, set at 95% CL on  $\sigma(HH)$  amounts to 97(53) times the SM expectation. The analysis also sets a limit on  $k_\lambda$ , amounting to  $-25.8(-14.4) < k_\lambda < 24.1(18.3)$ . The upper limits on  $\sigma(HH)$  in different EFT BM points set by this analysis vary from 1.7(1.0) to 6.2(3.9) pb.

### 5. $HH \rightarrow WW^*WW^*, WW^*\tau\tau, \tau\tau\tau\tau$ (multilepton)

This analysis [15] targets only the GGF production mode. Seven channels are considered based on the decay products of  $W$  bosons and  $\tau$  leptons. Events are divided into boosted and resolved categories depending on whether jets originating from hadronically decaying  $W$  bosons are reconstructed in one large radius jet or reconstructed separately in two small radius jets, respectively. Background contributions are estimated from simulation, except misidentified leptons and charge mis-identification which are estimated from data using a fake factor method [16]. A BDT is trained to separate signal from background. The BDT scores, along with two control regions for WZ and ZZ backgrounds, are used to extract the signal. This analysis sets an upper limit on  $HH$  production 21(19) times the SM expectation and a corresponding limit on  $\kappa_\lambda$  is set within the interval  $-6.9(-6.9) < \kappa_\lambda < 11.1(11.7)$ . Upper limits on  $\sigma(HH)$  in different EFT BM scenarios vary from 0.21(0.16) to 1.09(1.16) pb depending on event kinematics in different EFT BM points.

## 6. $VHH \rightarrow 4b$

This analysis [17] targets  $HH$  production in association with one vector boson ( $W$  or  $Z$  boson), where both  $H$  bosons decay to  $b\bar{b}$ . The analysis is performed in four final states: DL ( $Z \rightarrow ll$ ), SL ( $W \rightarrow l\nu$ ), FH ( $W/Z \rightarrow q\bar{q}$ ), MET ( $Z \rightarrow \nu\nu$ ). While a resolved category is analyzed in all final states, the boosted category is studied only in FH and MET final states. Large radius jets in the boosted category are identified and their mass is regressed by the ParticleNet [9] algorithm. A BDT is trained to separate regions in phase space sensitive to the couplings  $\kappa_\lambda$  and  $\kappa_{2V}$ . In each region, a separate BDT or neural network is trained to separate the  $VHH$  signal from background events. The observed (expected) upper limit on the  $VHH$  production cross section is 294(124) times the SM expectation at 95% CL. The corresponding constraint on  $k_\lambda$  amounts to  $-37.7(-30.1) < k_\lambda < 37.2(28.9)$ .

## 7. $HH \rightarrow bbWW^*$

This analysis [7] is performed both in GGF and VBF production modes and two final states are studied depending on the decay of the  $W$  bosons: DL (both  $W$ s:  $W \rightarrow l\nu$ ) and SL ( $W \rightarrow l\nu, W \rightarrow qq$ ). Events are classified into either boosted or resolved categories similar to  $HH \rightarrow bb\tau\tau$  analysis (Sec. 3). The resolved category is further split into 1, 2  $b$ -tagged categories depending on how many jets pass the medium working point of the DeepJet algorithm [18]. In the SL channel, at least one small radius jet originating from the hadronically decaying  $W$  boson is required. The background from misidentified leptons is estimated from data, using a fake factor method [16]. The contribution of Drell-Yan (DY) background in the DL final state is also measured from data. Other backgrounds are estimated from simulation. A Multiclassifier DNN training is used to separate the backgrounds from signal. The DNN distributions from all output nodes are used to extract the signals. The observed (expected) upper limit on  $HH$  production set by this analysis amounts to 14(18) times the SM expectation at 95% CL. A corresponding observed (expected) limit on  $\kappa_\lambda$  is set within the interval  $-7.2(-8.7) < \kappa_\lambda < 13.8(15.2)$ . The upper limits on  $\sigma(HH)$  in different EFT BM points vary from 0.16(0.2) to 2.3(2.2) pb.

## 8. Conclusion

The most recent results on  $\lambda_{HHH}$  have been presented using the full LHC Run 2 proton-proton data set recorded at  $\sqrt{s}=13$  TeV by the CMS experiment, corresponding to  $138 \text{ fb}^{-1}$  luminosity. The constraint on  $\sigma(HH)$  from the direct search in the  $HH$  analysis in five final states ( $bbZZ$ , multilepton,  $bb\gamma\gamma$ ,  $bb\tau\tau$ ,  $bbbb$ ) amounts to 3.4(2.5) times the SM expectation, analyzing the full Run 2 data (Fig. 2a). A corresponding limit on  $\kappa_\lambda$  is also set within the interval  $-1.24 < \kappa_\lambda < 6.49$  (Fig. 2b). Constraint on  $\lambda_{HHH}$  through indirect search of single  $H$  boson production at NLO correction is set within the interval  $-3.55 < \kappa_\lambda < 12.61$  [19]. The projection study of High Luminosity LHC (HL-LHC) is performed corresponding to  $3000 \text{ fb}^{-1}$  luminosity and at 14 TeV center-of-mass energy in five final states:  $bbbb$ ,  $bbZZ$  ( $ZZ \rightarrow 4l$ ),  $bb\gamma\gamma$ ,  $bb\tau\tau$  and  $bbVV$  ( $VV \rightarrow 2l$ ). In this projection  $\kappa_\lambda$  is constrained to lie within the interval  $-0.18 < \kappa_\lambda < 3.6$  at 95% CL (Fig. 3). Many improvements like adding new decay channels, leveraging modern machine learning techniques such as ParticleNet, using multi-classifier training and analyzing full Run 2 data, are considered in the analyses shown in Fig. 2. These improvements were not considered in the

projection study. By adding further decay channels, using improved machine learning techniques, more efficient triggers and further improvements, CMS is poised to make significant improvements on the measurement of  $\lambda_{HHH}$  by the end of LHC Run 3.

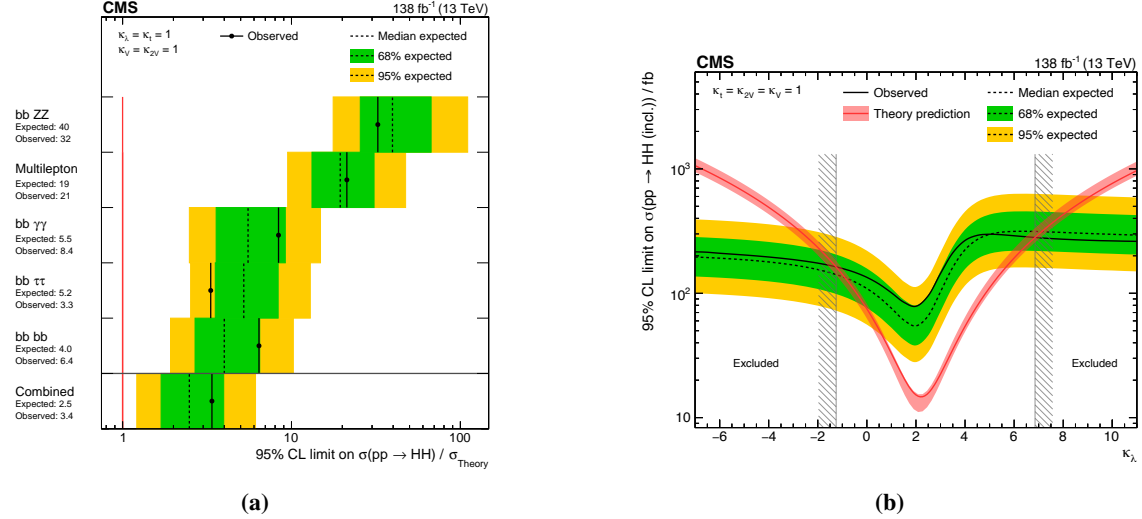


**Figure 2:** Observed and expected 95% CL upper limits on the  $HH$  production cross section with respect to the SM  $\sigma$  (a) and as a function of  $\kappa_\lambda$  (b) in  $bbZZ$ , multilepton,  $bb\gamma\gamma$ ,  $bb\tau\tau$ ,  $bbbb$  final states analyzing the full Run 2 data [19]

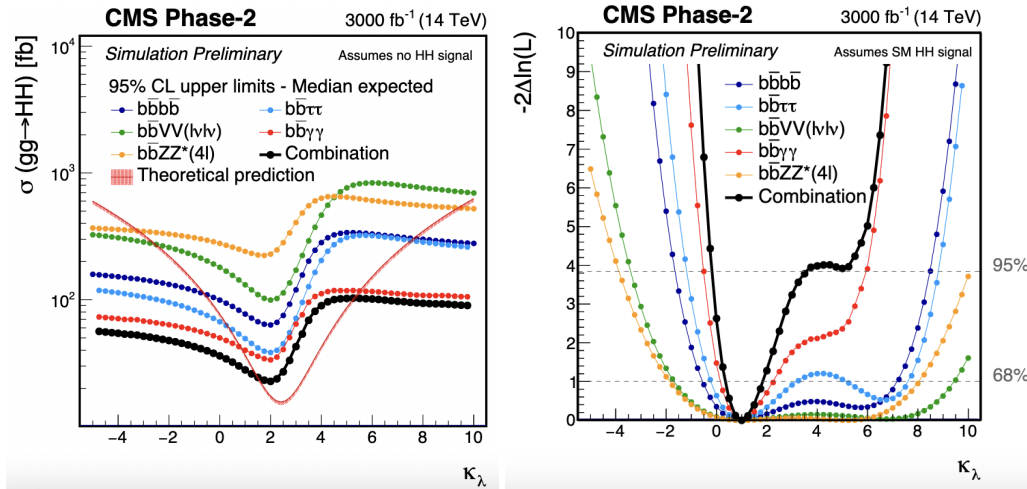


**Figure 3:** Upper limit at the 95% CL on the HH production cross section as a function of  $\kappa_\lambda$  (left) and expected likelihoodscan as a function of  $\kappa_\lambda$  in the HL-LHC projection study [20].

## References

- [1] CMS Collaboration, "Observation of a new boson at a mass of 125 GeV with the CMS experiment at the LHC" *Physics.Letters.B716(2012)30*
- [2] ATLAS Collaboration, "Observation of a new particle in the search for the Standard Model Higgs boson with the ATLAS detector at the LHC", *Phys.Lett.B716(2012)1 – 29*

- [3] CMS Collaboration, "Observation of a new boson with mass near 125 GeV in pp collisions at  $\sqrt{s}=7$  and 8 TeV", *JHEP06*, 081(2013)
- [4] Biagio Di Micco et al., "Higgs boson potential at colliders: Status and perspectives", *Rev.Phys.5*(2020)100045
- [5] Alexandra Carvalho et al., "Higgs pair production: choosing benchmarks with cluster analysis", *JHEP04*(2016)126
- [6] CMS Collaboration, "The CMS experiment at the CERN LHC", *JINST3*(2008)S08004.361p
- [7] CMS Collaboration, "Search for HH production in the bbWW decay mode", *CMS-PAS-HIG-21-005*
- [8] CMS Collaboration, "Search for Nonresonant Pair Production of Highly Energetic Higgs Bosons Decaying to Bottom Quarks", *Phys.Rev.Lett.131*, 041803
- [9] Huilin Qu and Loukas Gouskos, "Jet tagging via particle clouds", *Phys.Rev.D101*, 056019
- [10] CMS Collaboration, "Search for nonresonant Higgs boson pair production in final state with two bottom quarks and two tau leptons in proton-proton collisions at  $\sqrt{s}=13$  TeV", *Phys.Lett.B842*(2023)137531
- [11] CMS Collaboration, "Identification of hadronic tau lepton decays using a deep neural network", *JINST17*(2022)P07023
- [12] Lorenzo Bianchini et. al., "Reconstruction of the Higgs mass in  $H \rightarrow \tau\tau$  Events by Dynamical Likelihood techniques", *J.Phys. : Conf.Ser.513022035*
- [13] CMS Collaboration, "Search for nonresonant Higgs boson pair production in the  $WW\gamma\gamma$  channel in pp collisions at  $\sqrt{s} = 13$  TeV ", *CMS-PAS-HIG-21-014*
- [14] CMS Collaboration, "Search for nonresonant Higgs boson pair production in final states with two bottom quarks and two photons in proton-proton collisions at  $\sqrt{s} = 13\text{TeV}$ " *JHEP257*(2021)
- [15] CMS Collaboration, "Search for Higgs boson pairs decaying to  $WW^*WW^*$ ,  $WW^*\tau\tau$ , and  $\tau\tau\tau\tau$  in proton-proton collisions at  $\sqrt{s} = 13$  TeV", *JHEP07*(2023)095
- [16] CMS Collaboration, "Evidence for associated production of a Higgs boson with a top quark pair in final states with electrons, muons, and hadronically decaying  $\tau$  leptons at  $\sqrt{(s)} = 13\text{TeV}$ ", *JHEP66*(2018)
- [17] CMS Collaboration, "Search for Higgs boson pair production with one associated vector boson in proton-proton collisions at  $\sqrt{s} = 13\text{TeV}$ ", *CMS-PAS-HIG-22-006*
- [18] Emil Bols et.al., "Jet flavour classification using DeepJet" [arXiv:2008.10519](https://arxiv.org/abs/2008.10519)
- [19] CMS Collaboration, "A portrait of the Higgs boson by the CMS experiment ten years after the discovery", *Nature607*(2022)60 – 68
- [20] CERN Yellow Report, [doi.org/10.23731/CYRM-2019-007.221](https://doi.org/10.23731/CYRM-2019-007.221)